Cell

Aurora B-Mediated Abscission Checkpoint Protects against Tetraploidization

Patrick Steigemann,[1] Claudia Wurzenberger,[1] Michael H.A. Schmitz,[1] Michael Held,[1] Julien Guizetti,[1] Sandra Maar,[1] and Daniel W. Gerlich[1,*]
[1]Institute of Biochemistry, Swiss Institute of Technology Zurich (ETHZ), Schafmattstr. 18, CH-8093 Zurich, Switzerland
*Correspondence: daniel.gerlich@bc.biol.ethz.ch
DOI 10.1016/j.cell.2008.12.020

SUMMARY

Genomic abnormalities are often seen in tumor cells, and tetraploidization, which results from failures during cytokinesis, is presumed to be an early step in cancer formation. Here, we report a cell division control mechanism that prevents tetraploidization in human cells with perturbed chromosome segregation. First, we found that Aurora B inactivation promotes completion of cytokinesis by abscission. Chromosome bridges sustained Aurora B activity to posttelophase stages and thereby delayed abscission at stabilized intercellular canals. This was essential to suppress tetraploidization by furrow regression in a pathway further involving the phosphorylation of mitotic kinesin-like protein 1 (Mklp1). We propose that Aurora B is part of a sensor that responds to unsegregated chromatin at the cleavage site. Our study provides evidence that in human cells abscission is coordinated with the completion of chromosome segregation to protect against tetraploidization by furrow regression.

INTRODUCTION

Failures in cytokinesis can lead to tetraploidy (Caldwell et al., 2007; Fujiwara et al., 2005; Ganem et al., 2007; Uetake and Sluder, 2004), a state that has for a long time been suspected to contribute to cancer formation (Caldwell et al., 2007; Ganem et al., 2007), as recently demonstrated in a mouse model (Fujiwara et al., 2005). Faithful cytokinesis requires tight coordination with chromosome segregation (Eggert et al., 2006; Glotzer, 2005). Specifically, the completion of cytokinesis by abscission needs to await complete clearance of chromatin from the cleavage plane. While chromosome segregation normally completes early after anaphase onset, it can be severely delayed by lagging or bridged chromosomes. Such segregation defects have been estimated to occur in about 1% of dividing somatic cells, and at higher incidence in transformed cells (Cimini et al., 2003; Gisselsson et al., 2000). Chromosome bridges can result from dysfunctional telomeres (Maser and DePinho, 2002; Stewenius et al., 2005), DNA double-strand breaks (Acilan et al., 2007), or from misregulated chromosome cohesion (Chestukhin et al., 2003; Cimini et al., 2003) or decatenation (Chan et al., 2007). It is unclear how cells respond to chromosome bridges (Ganem et al., 2007; Mullins and Biesele, 1977; Weaver et al., 2006), and if any control mechanisms would ensure faithful abscission in the presence of chromosome bridges.

The regulation of abscission timing in animal cells is poorly defined, but may be related to a recently discovered pathway in budding yeast, termed NoCut (Norden et al., 2006). As part of this pathway, aurora kinase Ipl1 delays abscission in response to midspindle defects, which led to the hypothesis that it could monitor the completion of chromosome segregation for the control of abscission timing. It is not known if abscission timing is regulated at this level in higher eukaryotes.

The vertebrate homolog of Ipl1, Aurora B, is essential for mitosis and cytokinesis (Eggert et al., 2006; Ruchaud et al., 2007). Aurora B-dependent pathways regulating furrow ingression are well established. This includes Aurora B-dependent phosphorylation of mitotic kinesin-like protein 1 (Mklp1) (Guse et al., 2005; Neef et al., 2006). Following furrow ingression, Aurora B localizes to the midbody (Ruchaud et al., 2007), but its potential regulation of abscission timing has not been investigated. Mklp1 also localizes to the midbody (Guse et al., 2005; Neef et al., 2006), raising the possibility that Aurora B could regulate furrow ingression and abscission through common downstream effectors.

Aurora B is regulated at many levels (Ruchaud et al., 2007). To become active, it requires association with its coactivator INCENP. Its activity further depends on autophosphorylation at a threonine 232 residue in its activation loop (Yasui et al., 2004), and as part of the chromosome passenger complex, it needs to be targeted to distinct subcellular locations during mitotic progression.

Here, we established in vivo assays to investigate the regulation of abscission timing in human cells, and its coordination with the completion of chromosome segregation. We found that Aurora B inactivation at the midbody promotes abscission. Chromosome bridges delayed abscission and sustained Aurora B activity to posttelophase, which was essential to stabilize Mklp1 at the intercellular canal and to suppress furrow regression. Based on these data, we propose that Aurora B functions as part of a sensor that responds to unsegregated chromatin in the cleavage plane to control abscission timing and to protect missegregating cells against tetraploidization by furrow regression.

RESULTS

Chromatin Localized to the Cleavage Plane Can Lead to Spontaneous Furrow Regression

Previous studies reached controversial conclusions to which extent chromosome bridges cause tetraploidization by cytokinesis failure (Mullins and Biesele, 1977; Shi and King, 2005; Stewenius et al., 2005; Weaver et al., 2006). Because this could be due to the difficulty to reliably detect thin chromosome bridges by conventional wide field microscopy, we applied high resolution 3-D confocal time-lapse microscopy to monitor chromosome segregation and cleavage furrow ingression/regression in live cells. Using a HeLa cell line stably coexpressing markers for chromatin (H2B-mRFP [Keppler et al., 2006]), and plasma membrane (MyrPalm-mEGFP [Zacharias et al., 2002]), we found that cytokinetic furrow ingression always completed within 20 min after anaphase onset (n = 774), both in cells without chromosome bridges (n = 728), as well as in all cells with chromosome bridges (n = 46). Subsequent furrow regression occurred exclusively in cells with chromosome bridges (n = 16 out of 774 imaged dividing cells; Figure 1A and Movie S1 available with this article online). The sensitivity for bridge detection was validated by counterstaining with Hoechst (100% of Hoechst bridges were detectable by H2B-mRFP; n = 43; data not shown). These observations support the hypothesis that chromatin trapped in the cleavage plane is a main cause for spontaneous cytokinesis failure in tissue culture cells (Mullins and Biesele, 1977; Stewenius et al., 2005; Weaver et al., 2006). To compare the incidence of furrow regression in missegregating cells to the overall rate of tetraploidization, we next assayed the other known mechanisms that can lead to tetraploidization (Ganem et al., 2007). First, we assayed in the same dataset cell-to-cell fusion to neighboring nonsister cells, and spontaneous mitotic slippage (mitotic exit without chromosome segregation and cytokinesis; see Figure S1A). Neither process ever occurred in the movies of 774 dividing cells, indicating that these events must be extremely rare. Next, we probed for endoreplication (multiple rounds of replication without intermediate mitosis). By long-term confocal time-lapse imaging of HeLa cells stably expressing H2B-mRFP and the replication factory marker mEGFP-PCNA (Leonhardt et al., 2000), we found that cells always progressed from early to late S-phase replication foci patterns and subsequently entered mitosis, never entering a second S-phase without preceding mitosis (n = 173; assay shown in Figure S1B). Thus, spontaneous endoreplication must also be extremely rare, if present at all in HeLa cells. Finally, multinucleate cells always had thin DNA threads coated by the inner nuclear envelope marker LAP2 connecting their individual nuclei (Figure S1C; n = 20). This is consistent with their origin from furrow regression after chromosome bridging, but would not be expected to result from any other known process leading to tetraploidization. Together, our data suggest that furrow regression in response to chromosome bridges is the main cause for tetraploidization in HeLa cells.

Cells with Chromosome Bridges Proliferate Normally Unless They Regress the Cleavage Furrow

Consistent with previous studies (Fujiwara et al., 2005; Ganem et al., 2007; Shi and King, 2005), we found by long-term imaging of HeLa cells stably expressing H2B-mRFP over 80 hr that cells that regressed the furrow frequently entered abnormal mitosis, which impaired their proliferation (Figures 1B, 1D, 1E, and S1D, and Movies S2 and S4). Remarkably, the majority of cells with chromosome bridges (71%; n = 143) did not regress the furrow and proliferated at rates close to normally segregating cells (Figures 1C, 1D, and 1E, and Movies S3 and S4). We thus asked if chromosome bridges resolve shortly after anaphase onset to allow unperturbed abscission. Gradual thinning of chromosome bridges during mitotic exit limits their detection by time-lapse imaging of chromatin markers. However, the inner nuclear envelope marker EGFP-LAP2β (Muhlhausser and Kutay, 2007), which localized around chromatin from late anaphase on (Figure 2A and Movie S5), efficiently visualized chromosome bridges during subsequent cell cycle stages (LAP2β-bridges always correlated with chromosome bridges in high resolution still images; n = 10; Figure 2B). By time-lapse imaging, we found that the majority of chromosome bridges persisted long into interphase (76% for more than 5 hr; n = 46). The relatively low incidence of cleavage furrow regression is surprising with respect to the persistence of chromosome bridges, and could be due to a mechanism that delays abscission until eventual resolution of chromosome bridges.

Chromosome Bridges Delay Abscission

To address if chromosome bridges were correlated with delayed abscission, we probed for cytoplasmic continuity of postmitotic sister cells. HeLa cells expressing H2B-mCherry were scored for chromosome bridges during anaphase and then followed into interphase. A coexpressed photoactivatable GFP (PAGFP [Patterson and Lippincott-Schwartz, 2002]) was then photoactivated in one sister cell. Any subsequent increase of PAGFP fluorescence in the nonactivated sister cell reports on diffusion between the two cells, indicating that abscission had not taken place. While all normally segregating sister cells had undergone abscission 180 min after anaphase onset (n = 25 pairs of sister cells; Figure 2C), the majority of chromosome bridge-containing sister cells (86%, n = 29; Figure 2D) at that time were still connected by cytoplasmic canals that allowed PAGFP diffusion into the nonactivated sister cell. To test if in these cells abscission can occur at later interphase stages, we combined long-term time-lapse imaging of mRFP-LAP2β with the PAGFP assay (Figure S2). All cells that resolved the chromosome bridge had abscised prior to photoactivation (n = 14). In contrast, only a single out of 21 pairs of sister cells with intact chromosome bridges failed to exchange PAGFP. Together, these data demonstrate that chromosome bridges delay abscission.

Removal of Chromosome Bridges by Laser Microsurgery Leads to Abscission

To test if resolution of chromosome bridges directly leads to abscission, we established a protocol to remove chromosome bridges from the abscission site by intracellular laser microsurgery. Using HeLa cells stably coexpressing mRFP-LAP2β and MyrPalm-mEGFP as markers for the chromosome bridge and the plasma membrane, we first validated that laser cutting of the chromosome bridge at cytoplasmic regions close to the

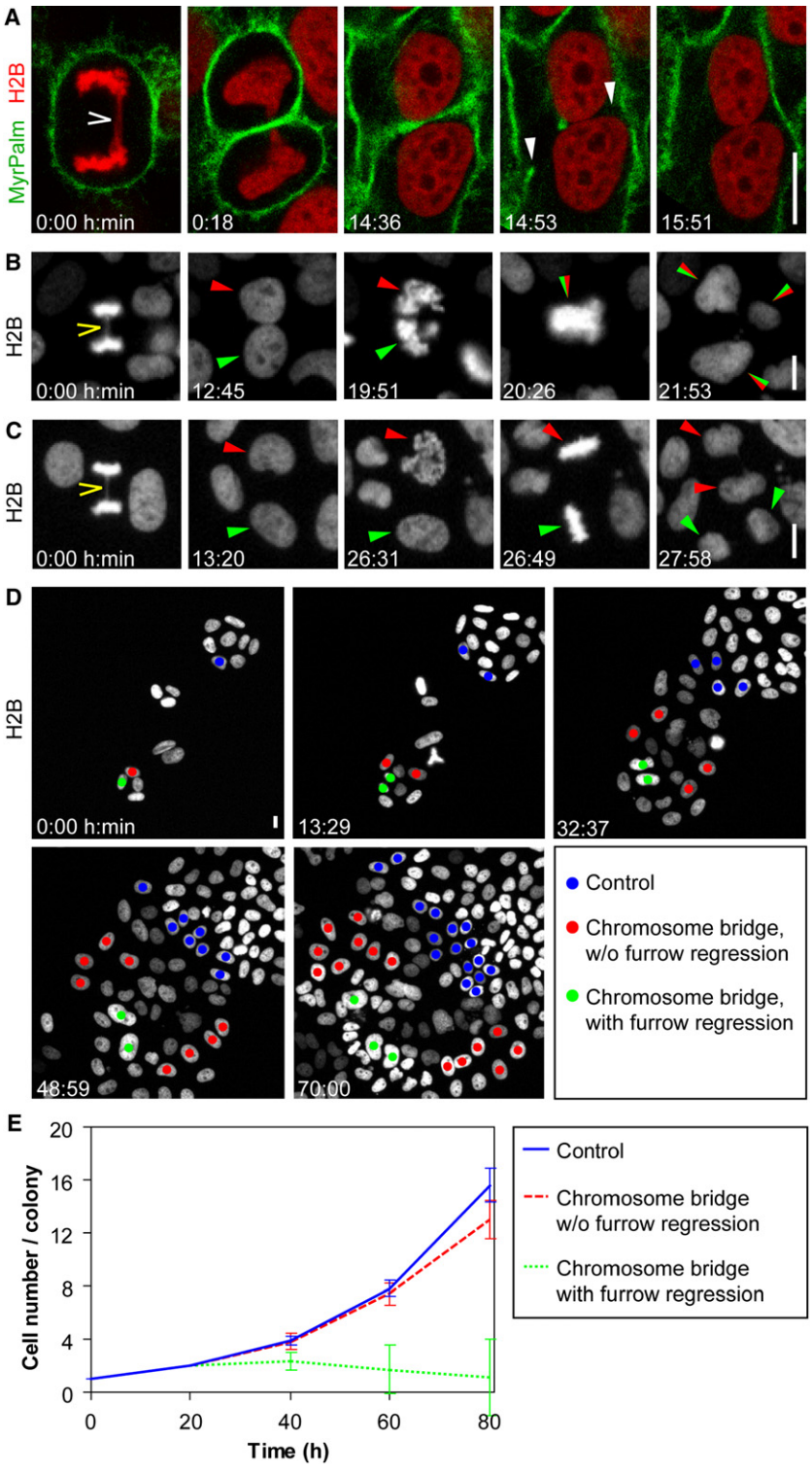

Figure 1. Effect of Chromosome Bridges on Abscission and Proliferation

(A) Chromosome bridge (0:00; open arrowhead) preceding cleavage furrow regression (14:53; arrowheads) in HeLa cell stably expressing markers for chromatin (H2B-mRFP) and plasma membrane (MyrPalm-mEGFP).

(B–E) Clonal proliferation studied by long-term imaging of H2B-mRFP expressing cells. (B) Chromosome bridge-containing cell (0:00; open arrowhead) whose daughter cells subsequently assembled a common metaphase plate (19:51; 20:26). This indicates cleavage furrow regression prior to mitotic entry, as validated in an independent experiment (see Figure S1D). (C) Chromosome bridge-containing cell (0:00; arrowhead), whose daughter cells enter the following mitosis separately (no cleavage furrow regression). Cell lineage was tracked according to arrowhead colors. (D) Clonal proliferation of control cells and cells with chromosome bridges. Lineages were manually tracked over time. (E) Quantitation of clonal proliferation as in (D).

Data are mean ± SD; n = 10 colonies per condition. Scale bars represent 10 μm.

nucleus (minimum distance from ingressed furrow 1.3 μm; mean distance 2.9 μm) did not affect the overall integrity of the sister cells (n = 9; Figure 2E). Next, we cut the chromosome bridge in cells stably coexpressing mRFP-LAP2β and PAGFP. In 6 out of 12 cells this led to complete removal of the bridge from the cytoplasmic canal connecting the sister cells (Figure 2F). By subsequent photoactivation of PAGFP in one sister cell and time-lapse imaging over 65 min we found that all cells with removed chromosome bridges had undergone abscission. This was unlikely due to simple mechanical separation of the entire sister cells by the laser cutting procedure, as the cutting path was at least 1.5 μm (mean distance 2.7 μm) displaced from the ingressed furrow, similar to the experiment shown in Figure 2E, which did not show any detectable changes in the morphology of the plasma membranes between sister cells 2 min (Figure 2E), as well as 30 min (data not shown) after laser microsurgery. To further test for the specificity of abscission in response to removal of the chromosome bridge, rather than potential unrelated cellular damage by the laser cutting procedure, we applied the same protocol with the laser cutting path slightly displaced from the chromosome bridge (Figure 2G). Only one out of 11 cells treated by this control procedure underwent abscission after laser microsurgery, as scored by the PAGFP assay. To exclude the possibility that the slightly different orientation of the laser cutting path relative to the abscission site affected the outcome of this experiment, we also tested if laser microsurgery would lead to abscission in telophase cells (Figure 2H). The cutting path was similar to that applied in cells with chromosomal bridges, with a minimum distance of 1.2 μm (mean distance 2.1 μm) from the ingressed furrow. In 12 out

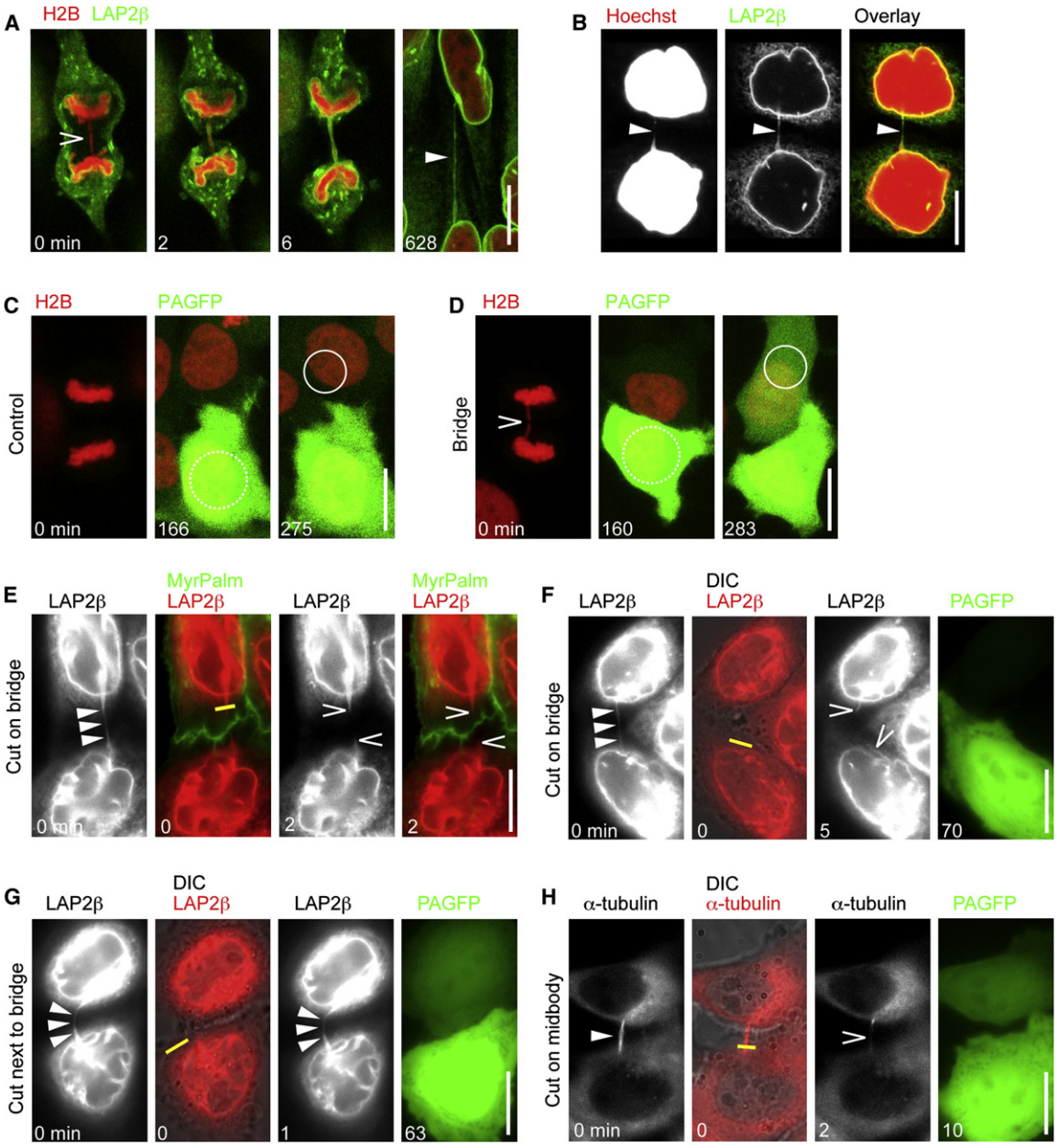

Figure 2. Chromosome Bridges Persist after Mitotic Exit and Delay Abscission

(A) Nuclear envelope assembly around chromosome bridge during late anaphase in HeLa cell expressing H2B-mRFP and EGFP-LAP2β. Open arrowhead at 0 min indicates chromosome bridge during early anaphase. Closed arrowhead at 628 min indicates chromosome bridge during interphase.

(B) Interphase LAP2β bridges contain chromatin. HeLa cells expressing mRFP-LAP2β were stained with Hoechst. Cells were synchronized to 15 hr after mitotic shake-off.

(C and D) Chromosome bridges delay abscission. Chromosome bridges were scored in HeLa cells stably expressing H2B-mCherry, and cells were followed by time-lapse imaging. Abscission was probed by photoactivation of PAGFP in one sister cell (dashed circles), and detection of PAGFP fluorescence approximately 2 hr later in the nonactivated sister cells (solid circles). (C) A normally segregating control cell showed no detectable PAGFP fluorescence in the nonactivated sister cell (275 min; solid circle), which indicates that abscission had taken place. (D) A cell containing a chromosome bridge (open arrowhead) showed PAGFP fluorescence in the nonactivated sister cell (283 min; solid circle), and had thus not abscised.

(E) Removal of the chromosome bridge by laser microsurgery (along the yellow line) does not perturb normal cell membrane morphology, as visualized in HeLa cells stably expressing MyrPalm-mEGFP and mRFP-LAP2β.

(F and G) Removal of chromosome bridge from the cleavage site leads to abscission. Chromosome bridges (arrowheads) were visualized in HeLa cells stably expressing mRFP-LAP2β and PAGFP. Laser microsurgery was close to the nucleus of one sister cell as indicated by yellow lines. Photoactivation of PAGFP in one sister cell was 5 min after laser cutting and was repeated in 10 min intervals during subsequent time-lapse imaging. (F) Removal of the bridge (5 min; open arrowheads mark tips after cutting) led to abscission (70 min), (G) Cutting at cytoplasmic regions adjacent to the chromatin bridge did not lead to abscission (63 min).

of 13 pairs of sister cells, PAGFP still exchanged 10 min after laser microsurgery, demonstrating that the laser microsurgery procedure per se does not cause abscission. We conclude that removal of chromatin from the cleavage plane leads to abscission.

Conversion of Midbodies into Stable Intercellular Canals

The ingressed cleavage furrow is normally anchored at the midbody. The disassembly of midbody microtubule bundles defines the end of telophase, which normally coincides with abscission (see below). Midbody disassembly proceeds by sequential disassembly of microtubule bundles on either side of a central midbody region, which subsequently persists as a midbody remnant (Figures S3A and S3B). We were thus surprised to note that despite of the abscission delay, chromosome bridge-containing HeLa cells disassembled midbody microtubule bundles already 60 ± 9 min (mean ± SD; n = 19; Figure 3A and Movie S6) after furrow ingression, similar to normally segregating cells (60 ± 10 min; n = 12; Figure S3B and Movie S7). To investigate if other cytoskeletal structures could contribute to the stabilization of intercellular canals in cells with chromosome bridges, we visualized actin in vivo using a HeLa cell line stably coexpressing actin-EGFP and H2B-mRFP. We found that in normally segregating cells actin enriched at the ingressing cleavage furrow, where it remained until 61 ± 11 min (n = 12; Figure S3C and Movie S8). The disappearance of actin-EGFP accumulations from the ingressed furrow thus correlated with the time of midbody microtubule disassembly and abscission (compare with Figures S3C, 5E, and 5F). Cells containing chromosome bridges did not disassemble actin-EGFP at that time, but instead accumulated actin-EGFP at two prominent patches on either side of the cytoplasmic canal (Figure 3B, Movie S9; patches detected in 90% of chromosome bridge-containing cells; n = 166; never in cells without chromosome bridges; n = 45). Actin patches could also be visualized by phalloidin (Figure S3D) and remained stable throughout interphase (Figure S3E and Movie S10), and disappeared only when chromosome bridges resolved (Figures 3C, S3F, and Movie S11; n = 18), or the cleavage furrow regressed (Figure 3D and Movie S12; n = 46). Thus, missegregating cells delay abscission at stable actin-rich canals.

Mechanical Barriers Do Not Induce Stable Intercellular Canals

Abscission delay and assembly of stable intercellular canals induced by chromosome bridges could be a constitutive cellular response to the presence of a mechanical barrier. Alternatively, it could specifically depend on the presence of chromatin at the cleavage site. To discriminate between these possibilities, we introduced mechanical barriers at the cleavage site that did not contain chromatin. Asbestos fibers, which have similar dimensions as chromosome bridges (Fig. S4A, B), efficiently incorporate into dividing cells (Jensen et al., 1996). Localization of asbestos fibers to cytoplasmic regions close to the ingressing cleavage furrow did not perturb furrow ingression (n = 84; Figure 4A and Movie S13) and midbody assembly (n = 23; Figure 4B). Cells with asbestos fibers at the ingressed furrow never contained actin accumulations at the intercellular canal (Figure 4C; n = 13; compare Figure S3D), and frequently regressed the furrow very early after telophase (62% within 3 hr after furrow ingression; n = 84; detected by confocal time-lapse imaging; Figure 4A and Movie S13). However, furrow regression never occurred when intracellular asbestos fibers were not trapped by the ingressed furrow (n = 42; Figure S4C), demonstrating that rapid furrow regression depended on the specific localization of asbestos fibers. Together, these data indicate that mechanical blockage at the abscission site is not sufficient to sustain a stable intercellular canal.

Aurora B Controls Abscission Timing

The regulation of abscission timing in animal cells is unknown, but in *S. cerevisiae* depends on the inactivation of the aurora kinase Ipl1 (Norden et al., 2006). We thus investigated if this function is conserved in the mammalian Ipl1 homolog, Aurora B. Aurora B did not change its localization upon midbody microtubule disassembly (Figure S5A), which normally coincides with abscission (see below). It persisted at high levels on the midbody remnant, a structure that becomes visible after abscission (detected on midbody remnant by immunofluorescence in 49/50 cells; Figures 5A and 5B; by time-lapse imaging of Aurora B-EGFP during midbody disassembly; Figure S5A). It is therefore unlikely that sub-cellular localization changes or degradation of Aurora B contribute to abscission control. Aurora B activity depends on phosphorylation of a T232 residue (Yasui et al., 2004). Using an antibody specifically recognizing phospho-T232-Aurora B, we found midbody-localized Aurora B always highly phosphorylated (n = 20; Figure 5C), suggesting that Aurora B remains active throughout entire telophase. The antibody was specific, as inhibition of Aurora B by ZM1 (Girdler et al., 2006) removed all detectable phospho-T232 Aurora B from late midbodies (Fig. S5B-C). Midbody remnants never contained significant amounts of phospho-T232-Aurora B (0.8 ± 1.3% of telophase levels; n = 20; Figure 5D). The correlation of Aurora B dephosphorylation with midbody microtubule disassembly suggests that Aurora B inactivation may provide a trigger for abscission. To directly test this, we examined the effect of premature Aurora B inactivation during telophase in HeLa cells stably coexpressing mCherry-α-tubulin and PAGFP. By repetitive photoactivation of PAGFP in one postmitotic sister cell, and measuring increase of fluorescence in the other sister cell over time, we determined the precise timing of abscission (Figures 5E–5G, and Movie S14). In normally segregating HeLa cells abscission occurred 60 ± 10 min (mean ± SD; n = 12) after complete cleavage furrow ingression. This coincided with disassembly of midbody microtubule bundles (60 ± 9 min; mean ± SD;

(H) Laser microsurgery at the midbody does not induce abscission. Laser microsurgery (along the yellow line) was applied to telophase HeLa cells stably coexpressing mCherry-α-tubulin and PAGFP. Ablation of one side of the midbody with identical settings as in the experiments shown in (E–G) did not induce abscission 10 min after microsurgery.

Scale bars represent 10 μm.

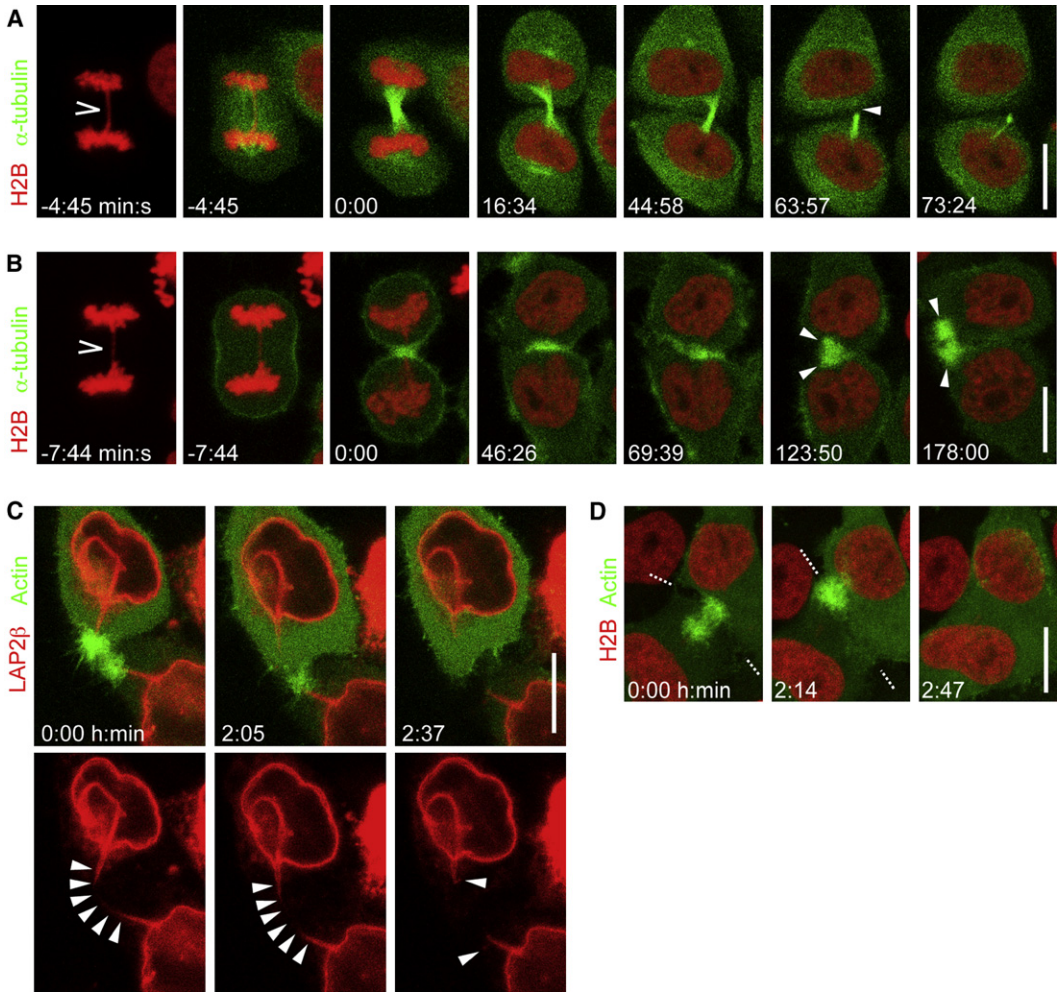

Figure 3. Delayed Abscission Occurs at Stable Actin-Rich Intercellular Canals

(A) Normal midbody microtubule disassembly (arrowhead; 63:57) in HeLa cell stably expressing mEGFP-α-tubulin and H2B-mRFP with chromosome bridge (open arrowhead; −4:45).

(B) Assembly of actin patches (arrowheads, 123:50; 178:00) in HeLa cell stably expressing H2B-mCherry and actin-EGFP containing chromosome bridge (open arrowhead; −7:44).

(C) Actin patches disassemble when chromosome bridges resolve (2:05 - 2:37; arrowheads). Time-lapse recording of a HeLa cell expressing mRFP-LAP2β and actin-EGFP.

(D) Disassembly of actin-patches during furrow regression (2:47). HeLa cells stably expressing H2B-mCherry and actin-EGFP were scored for chromosome bridges during anaphase. Dashed lines indicate the position of the ingressed furrow.

Scale bars represent 10 μm.

n = 19). When cells that had completed furrow ingression were treated with the Aurora kinase inhibitor Hesperadin (Hauf et al., 2003), they abscised significantly earlier (44 ± 7 min; mean ± SD; n = 14; 2-tailed Mann-Whitney U-test at $\alpha = 0.01$; $p < 0.001$; Figure 5G), again coincident with premature midbody microtubule disassembly (41 ± 6; mean ± SD; n = 30; $p < 0.001$). Similar data were obtained with a different Aurora B inhibitor, ZM1 (Girdler et al., 2006) (Figure 5G), and in normal rat kidney (NRK), and in noncancer human retinal pigment epithelial (hTERT-RPE1) cells (Figure 5H), in which the expression levels of Aurora B were similar to HeLa cells (Figure S6E). We conclude that Aurora B inactivation promotes abscission in animal cells.

Chromosome Bridges Sustain Aurora B Activity to Posttelophase Stages

To test if Aurora B could also control delayed abscission in mis-segregating cells, we investigated its localization and activity by immunofluorescence in HeLa cells with chromosome bridges synchronized to 3 hr after mitotic shake-off. We staged cells as posttelophase based on disassembled midbody microtubule bundles (see above). Aurora B localized to a single narrow ring at the site where the chromosome bridge passed through the ingressed furrow (n = 35; Figures 6A and 6D; Movie S15). In these rings, Aurora B was highly phosphorylated at T232 (n = 21; Figure 6B), in contrast to midbody remnants in posttelophase cells without chromosome bridges (see above and compare

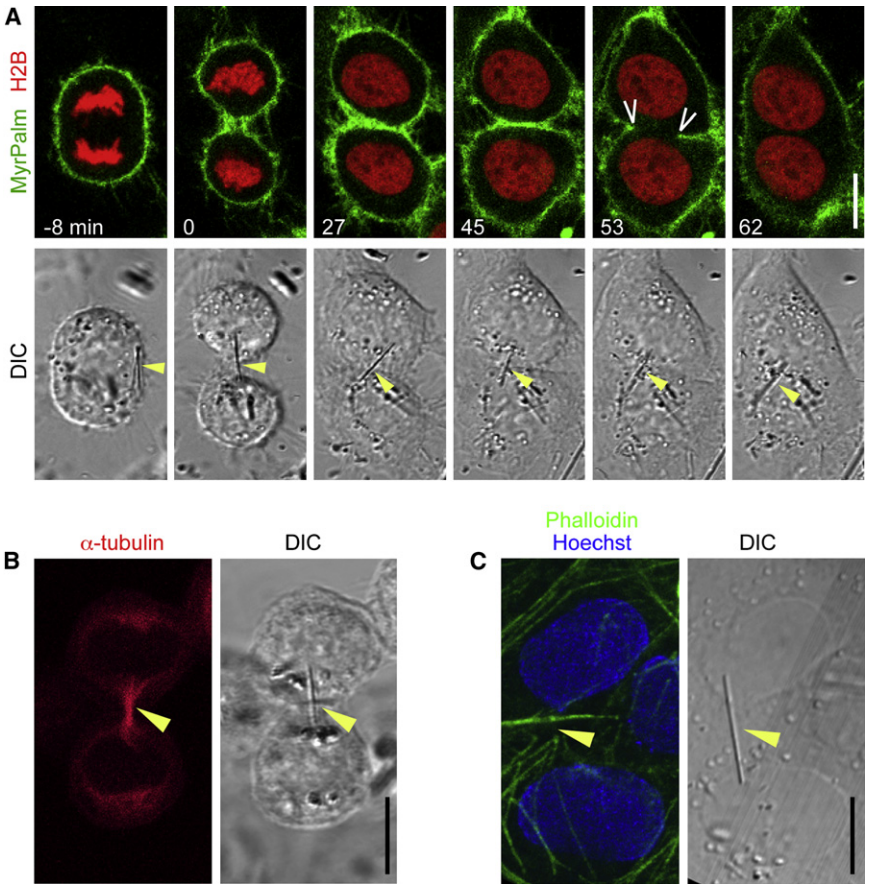

Figure 4. Mechanical Barriers to Abscission Do Not Stabilize Intercellular Canals after Telophase

(A) Asbestos fibers (arrowheads) do not interfere with furrow ingression and anchoring during telophase (0 - 45 min), but lead to furrow regression during interphase (open arrowheads; 53 min) in HeLa cells stably expressing H2B-mRFP and MyrPalm-mEGFP.

(B) Midbody morphology is unaffected by asbestos fiber (arrowhead) passing through the ingressed furrow in a cell stably expressing mRFP-α–tubulin.

(C) Asbestos fibers (arrowhead) do not induce actin patches at the intercellular canal in interphase HeLa cells. Actin was visualized by Phalloidin staining in fixed cells (compare Figure S3D). Scale bars represent 10 μm.

Figure 5D). High levels of T232 phosphorylation were also detected at chromosome bridges in 39 out of 40 unsynchronized interphase cells, indicating that Aurora B also remains phosphorylated throughout later stages of interphase in cells with chromosome bridges. Phosphorylated T232-Aurora B was also present at rings around interphase chromosome bridges in NRK and hTERT-RPE1 cells (Figures S6A and S6B). The Aurora B coactivator INCENP also localized at rings around interphase chromosome bridges (n = 19 of 20 cells; Figure 6C).

Inhibition of Aurora B by ZM1 reduced the levels of T232 phosphorylation at chromosome bridges in HeLa cells to 48 ± 34% (n = 25; synchronized to 3 hr postmitotic shake-off). Because the phospho-T232 antibody did not cross-react at detectable levels with unphosphorylated Aurora B during telophase (compare Figures S5B and S5C), this suggests that at interphase rings in cells with chromosome bridges, phospho-T232 did not exclusively depend on Aurora B autophosphorylation. Together, these data indicate that chromosome bridges sustain Aurora B activity to posttelophase stages.

We next addressed the dynamics of Aurora B within the ring by fluorescence recovery after photobleaching (FRAP) in HeLa cells expressing mRFP-LAP2β and EGFP-tagged Aurora B (Yan et al., 2005). Aurora B-EGFP fluorescence recovered to 32 ± 9% (mean ± SEM; n = 7) within 45 min after complete photobleaching of the ring (Figures 6E and 6F), indicating that Aurora B bound dynamically to the ring and constantly exchanged with the cytoplasm. To probe if it could gain access to chromatin inside of the nuclear envelope, we next investigated nuclear-cytoplasmic shuttling of Aurora B-EGFP in interphase HeLa cells stably coexpressing Aurora B-EGFP and H2B-mCherry. For this, we repetitively photobleached at a cytoplasmic region and probed for changes of fluorescence intensity inside the nucleus (Figure 6G). As cytoplasmic photobleaching rapidly depleted nuclear fluorescence of Aurora B-EGFP (n = 7; Figure 6H), we conclude that Aurora B can efficiently cross the nuclear envelope.

Aurora B Protects Missegregating Cells against Cleavage Furrow Regression

We next examined the function of prolonged Aurora B activity in cells with chromosome bridges. One possibility is that premature inactivation of Aurora B could induce abscission followed by cutting of the chromosome bridge and DNA damage, similar to the phenotype observed in Ipl1 deficient budding yeast (Norden et al., 2006). Alternatively, the cytokinetic machinery in animal cells might not be able to cut through chromosome bridges. If this was the case, prematurely triggered abscission could fail and lead to in increased rates of cleavage furrow regression.

We therefore tested if Aurora B inhibition in missegregating cells promoted cutting through chromosome bridges or furrow regression. Aurora B inhibition had no influence on the incidence of chromosome bridge resolution during 14 hr time-lapse imaging of HeLa cells stably coexpressing EGFP-LAP2β and H2B-mRFP (19% in control, n = 36; 15% in Hesperadin or ZM1-treated cells, n = 27). In contrast, Aurora B inhibition after complete furrow ingression significantly (Fisher's exact test at $\alpha = 0.01$; $p < 0.001$) raised the incidence of cleavage furrow regression in chromosome bridge-containing cells from 33% in control cells (n = 98) to 81% in cells treated with Hesperadin (n = 79), and 66% in ZM1 treated cells (n = 53; Figure 6I). With 76% of anaphase chromosome bridges persisting throughout

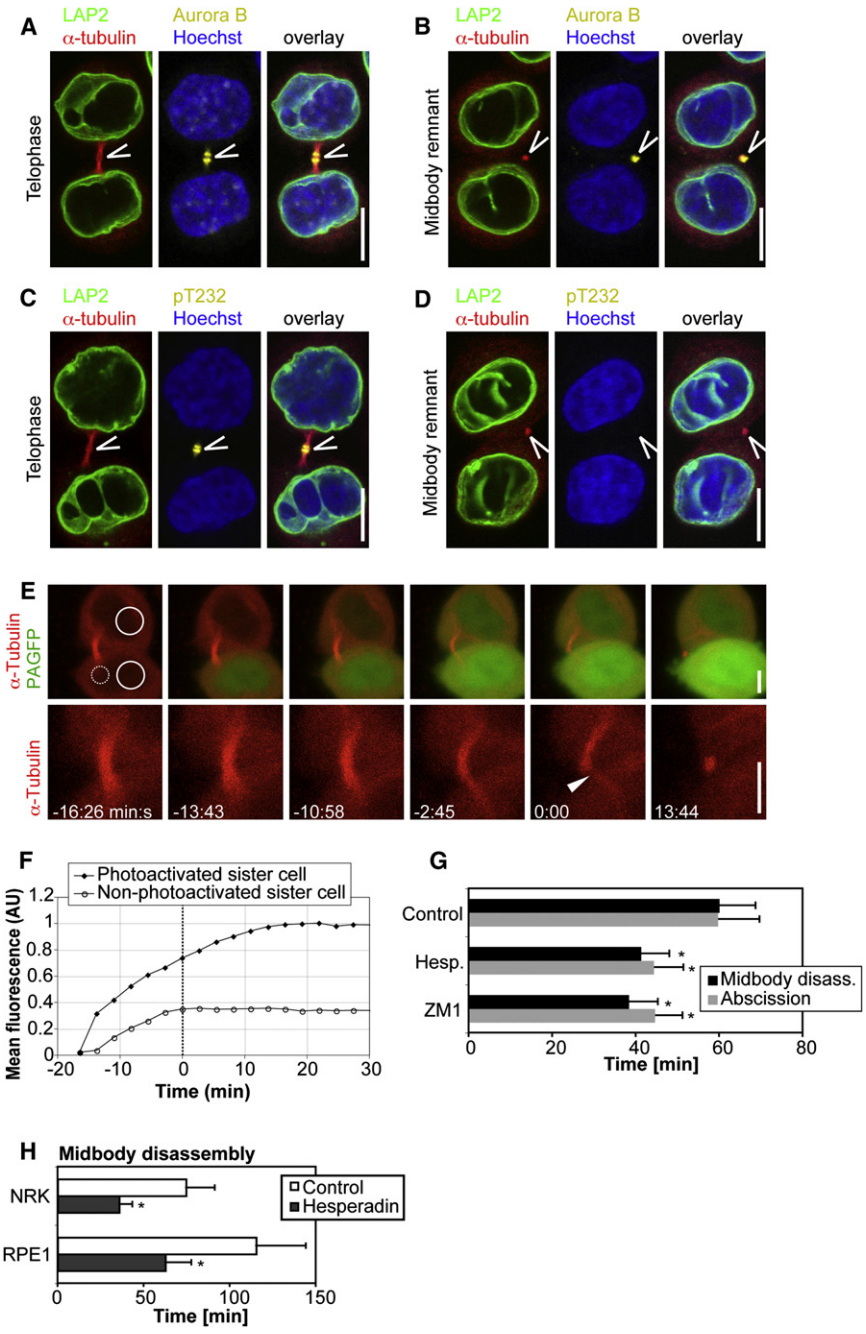

Figure 5. Aurora B Controls Abscission Timing

(A–D) Immunofluorescence in HeLa cells stably expressing mRFP-α-tubulin to visualize the telophase midbody (open arrowheads in [A] and [C]), and the midbody remnant after abscission (open arrowheads in [B] and [D]). Cells did not contain chromosome bridges, as validated by an antibody against LAP2. Antibodies against Aurora B, and phospho-T232-Aurora B were as indicated in the individual panels. Scale bars represent 10 μm.

(E and F) Assay for abscission timing. (E) Abscission timing probed by repetitive photoactivation of PAGFP in region marked by dashed circle in a HeLa cell expressing mCherry-α-tubulin and PAGFP. Arrowhead indicates onset of midbody microtubule disassembly (t = 0:00). Scale bars represent 5 μm. (F) Mean PAGFP fluorescence was measured in both sister cells as indicated by solid circles in (E). Abscission was determined by the stop in fluorescence increase in the nonactivated sister cell (0:00).

(G) Timing from complete furrow ingression until midbody microtubule disassembly and abscission was measured by the assays depicted in (E and F). Cells were treated after complete furrow ingression with Hesperadin, ZM1, or DMSO for control.

(H) Timing from midbody formation until midbody microtubule disassembly in NRK and hTERT-RPE1 cells.

Bars represent mean of at least three experiments, error bars indicate SD, * indicates significant differences to control tested by 2-tailed Mann-Whitney U-test at a = 0.01.

interphase (as shown above; Figure 2A) these data indicate that most if not all cells with persistent chromosome bridges undergo cleavage furrow regression upon Aurora B inhibition. This cannot be due to a general unspecific cellular response to kinase inhibitors, as neither Cdk1, nor MAPK inhibition during telophase significantly changed the incidence of furrow regression in cells with chromosome bridges: 31%, n = 35 after Cdk1 inhibition by RO-3306; 38%, n = 47 after MAPK inhibition by SB203580 ($p > 0.1$ for both conditions compared to control, tested by Fisher's exact test). Importantly, Aurora B inhibition after complete furrow ingression never induced furrow regression in normally segregating cells (n = 50). This demonstrates that after complete furrow ingression Aurora B has for main function to prevent cleavage furrow regression in cells with chromosome bridges.

Aurora B Phosphorylates and Stabilizes Mklp1 at the Intercellular Canal

A key requirement to prevent cleavage furrow regression is the maintenance of a cortically anchored furrow at a stable intercellular canal. Mklp1 has been proposed as such an anchoring factor during telophase (Guse et al., 2005; Neef et al., 2006). We thus addressed its role in interphase cells with chromosome bridges. Using immunofluorescence on HeLa cells synchronized to 3 hr after mitotic shake-off, we found Mklp1 localized to a narrow ring at the cytoplasmic canal connecting chromosome bridge-containing sister cells, similar to Aurora B (n = 36; Figure 7A; compare Figure 6A). Using a phospho-specific antibody (Neef et al., 2006), we found Mklp1 in these rings phosphorylated at a S911 residue (n = 11 for HeLa cells; Figure 7A; for hTERT-RPE1 and NRK cells see Fig. S6C, D). Inhibition of Aurora B by ZM1 in chromosome bridge-containing HeLa cells after

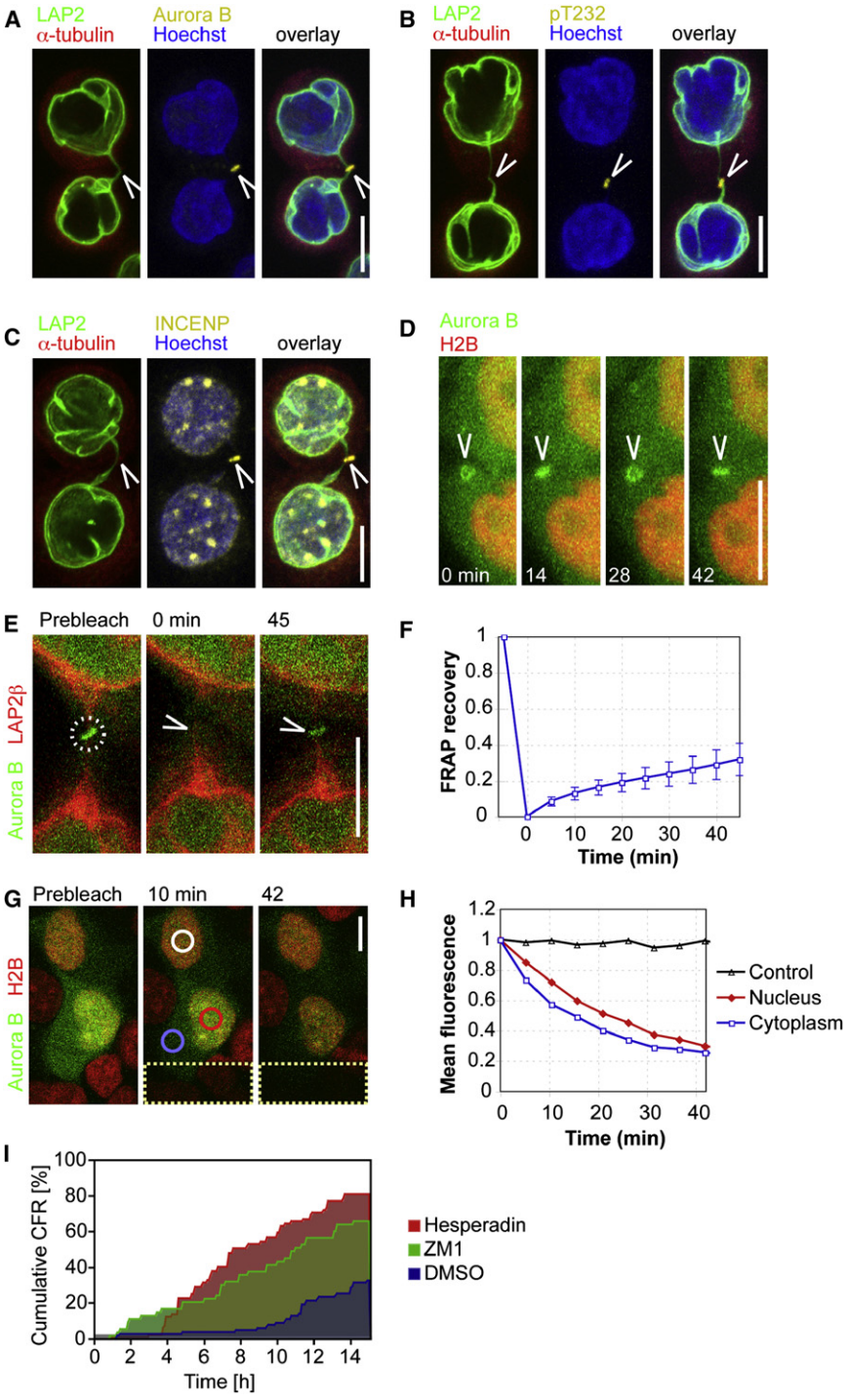

Figure 6. In Posttelophase Cells with Chromosome Bridges, Aurora B Remains Active to Protect against Tetraploidization by Furrow Regression

(A–C) Immunofluorescence stainings of HeLa cells stably expressing mRFP-α-tubulin. Chromosome bridges were detected by an antibody against LAP2. Staining with antibodies against Aurora B (A), phospho-T232 Aurora B (B), and INCENP (C). Arrowheads mark the site where the LAP2 bridge passes through the ingressed furrow.

(D) Aurora B-EGFP localized to a ring (arrowheads) in interphase HeLa cell stably expressing H2B-mCherry and Aurora B-EGFP.

(E and F) Dynamic association of Aurora B with the ring. (E) HeLa cells expressing mRFP-LAP2β and Aurora B-EGFP were photobleached in regions as indicated by the dashed circle. Open arrowheads mark the position where the ring previously localized, immediately after photobleaching (0 min) and after 45 min. (F) Quantitation of fluorescence recovery in the bleached region. Time point 0 corresponds to the frame immediately after photobleaching. Data are mean ± SEM (n = 7).

(G and H) Nuclear-cytoplasmic shuttling of Aurora B. (G) Repetitive photobleaching of Aurora B-EGFP in cytoplasmic regions (dashed area) of HeLa cells stably coexpressing Aurora B-EGFP and H2B-mCherry also depleted Aurora B-EGFP fluorescence both in the cytoplasm (blue circle), and in the nucleus (red circle). Nuclear fluorescence of Aurora B-EGFP in a neighboring cell (white circle) remained constant. (H) Quantification of fluorescence in regions similar to those indicated in (G). The mean normalized to the prebleach frame from seven experiments is plotted.

(I) Aurora B inhibition during telophase causes tetraploidization in chromosome bridge-containing cells. H2B-mRFP and MyrPalm-mEGFP expressing HeLa cells were scored for chromosome bridges during anaphase (compare Figure 1A), and treated with DMSO (Control), Hesperadin, or ZM1 in telophase (t = 0). Cleavage furrow regression (CFR) was detected during subsequent 15 hr time-lapse recording.

Scale bars represent 10 μm.

complete furrow ingression reduced phospho-S911 levels at the ring to 3.8 ± 4.4% (n = 11; Figure 7B). Aurora B inhibition also led to gradual loss of Mklp1 from the ring around chromosome bridges, which we quantitated in time-lapse movies of cells coexpressing Mklp1-YFP and H2B-mRFP (n = 15; Figures 7C and 7D). Together, these data establish Mklp1 as a prime downstream effector candidate of Aurora B for stabilization of the ingressed furrow in chromosome bridge-containing posttelophase cells.

DISCUSSION

Our study provides first evidence that abscission timing in animal cells depends on the completion of chromosome segregation, which is necessary to prevent tetraploidization by furrow regression.

Our data support the view that chromatin trapped in the cleavage plane is the major cause for spontaneous tetraploidization in cultured cells (Weaver et al., 2006). However, we found that most cells with chromosome bridges suppressed furrow regression and continued to proliferate normally. Our study

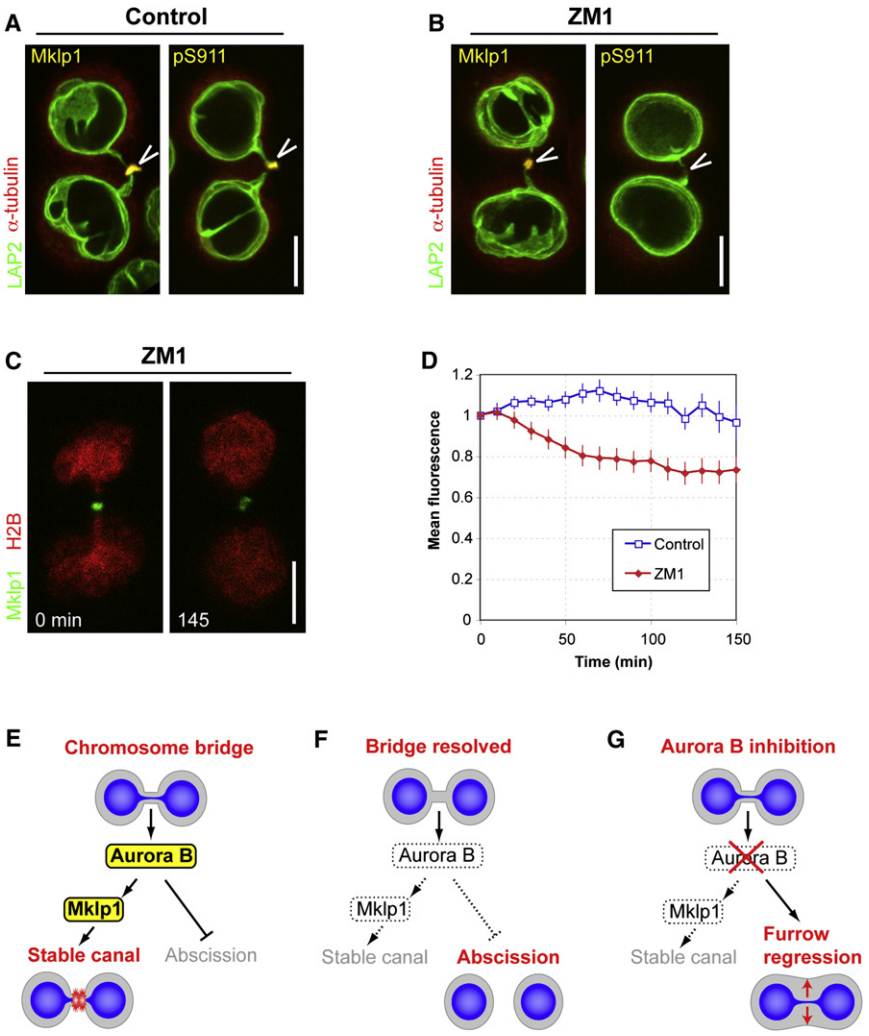

Figure 7. Aurora B-Dependent Phosphorylation and Stabilization of Mklp1

(A and B) Aurora B-dependent phosphorylation of Mklp1. Immunofluorescence in HeLa cells stably expressing mRFP-α-tubulin to validate by disassembled midbody microtubules that cells were in interphase. Chromosome bridges were detected by an antibody against LAP2. Antibodies detecting Mklp1, and phospho-S911-Mklp1 were used as indicated. (A) Cells were synchronized by mitotic shake-off, and fixed after 3 hr. (B) Cells were treated with ZM1 15 min after mitotic shake-off and fixed after 3 hr.

(C and D) Aurora B inhibition destabilizes Mklp1-YFP at stable cytoplasmic canals in cells with chromosome bridges. (C) HeLa cells expressing H2B-mCherry and Mklp1-YFP were scored for chromosome bridges in anaphase. ZM1 was added after complete furrow ingression (0 min), and cells were followed by time-lapse imaging. (D) Quantitation of mean Mklp1-YFP fluorescence at the ring in cells treated with ZM1 as in (C), or DMSO-treated control cells. Mean ± SEM of 14 (ZM1), or 10 (Control) cells is plotted.

(E–G) Model for the function and regulation of Aurora B in cells with chromosome bridges. Active states are highlighted in yellow. (E) The presence of a chromosome bridge sustains Aurora B activity to posttelophase stages, which leads to Mklp1 phosphorylation, stabilization of the intercellular canal, and delays abscission. (F) Resolution of chromosome bridge leads to removal of chromatin from the cleavage site, and inactivation of Aurora B. This destabilizes the intercellular canal and leads to abscission. (G) Chemical inhibition of Aurora B in the presence of a chromosome bridge destabilizes the intercellular canal and leads to tetraploidization by furrow regression. Scale bars represent 10 μm.

provides a mechanistic explanation for this: these missegregating cells stabilized the ingressed furrow and delayed abscission to posttelophase stages. Removal of chromosome bridges either by spontaneous resolution or by laser microsurgery resulted in rapid abscission. On the other hand, when abscission was mechanically blocked by asbestos fibers cells did not maintain an ingressed furrow during interphase. Together, this suggests a specific signal provided by chromatin at the cleavage site to stabilize the ingressed furrow for delayed abscission.

Our data lead us to propose a model with Aurora B as a key regulator of abscission timing, which responds to unsegregated chromatin (Figures 7E–7G). Aurora B inactivation probably involving dephosphorylation by a yet unknown mechanism normally promotes abscission about one hour after anaphase onset. The presence of chromosome bridges prevents Aurora B inactivation, and leads to its re-localization to a narrow ring at the intercellular canal upon midbody disassembly. This stabilizes the intercellular canal for delayed abscission. Premature inactivation of Aurora B in cells with chromosome bridges leads to furrow regression, likely due to premature destabilization of the intercellular canal at a stage that is not yet compatible with abscission.

Aurora B phosphorylation at intercellular canals does not exclusively depend on its auto-activation, since inhibition of Aurora B at this stage did not completely remove phospho-T232 at intercellular canals. This predicts that Aurora B could be activated by additional kinases, putatively localized on unsegregated chromatin at the cleavage site. Alternatively, chromosome bridges could counteract dephosphorylation of Aurora B by inhibitory phosphatases. Either possibility would provide an intriguing explanation how Aurora B could function in a chromatin sensor. Recent in vitro studies demonstrated that Aurora B can be regulated by chromatin (Kelly et al., 2007; Rosasco-Nitcher et al., 2008). Because ring-localized Aurora B can access chromatin by nuclear-cytoplasmic shuttling, this may provide a starting point to investigate the mechanistic details how chromosome bridges could sustain Aurora B activity.

Consistent with previous studies on earlier cytokinetic stages (Neef et al., 2006), we found that Aurora B phosphorylates S911 of Mklp1 at the stable cytoplasmic canal connecting posttelophase sister cells, and active Aurora B was required to maintain stable levels of Mklp1 at this localization. Based on the proposed function of Mklp1 to stabilize the midbody and anchor the

ingressed furrow during telophase (Guse et al., 2005), it is conceivable to speculate that Mklp1 could also contribute to the stability of the posttelophase canal. It will be interesting to test this once time-controlled perturbation of Mklp1 becomes possible, e.g., by specific small molecule inhibitors.

The abscission delay in response to chromosome segregation errors by Aurora B-like kinases is evolutionary conserved in budding yeast ((Norden et al., 2006) and Y. Barral and M. Mendoza, personal communication). In contrast to yeast, the main function of the abscission delay in human cells is to prevent tetraploidization, rather than chromosome breakage. This suggests that the mammalian abscission machinery is incapable of cutting through chromatin, which might be due to the lack of a stabilizing septum or the higher condensation state of human chromosomes as compared to their yeast counterparts.

In conclusion, our study defines a new regulatory mechanism for abscission in animal cells that prevents tetraploidization by furrow regression in response to chromosome segregation defects. At an estimated incidence of chromosome bridges in normal somatic tissues of about 1% (Cimini et al., 2003; Gisselsson et al., 2000), this likely is an essential requirement for organismal development. Because of the oncogenic potential of tetraploidization (Fujiwara et al., 2005; Ganem et al., 2007), it could also reduce the risk of cancer in aging tissues, where the incidence of chromosome bridges increases due to telomere attrition (Chin et al., 2004; Maser and DePinho, 2002; Stewenius et al., 2005). However, how tetraploidization of individual cells contributes to aneuploidy in cell populations and cancer formation will need further thorough investigation. Aurora B has recently received significant attention as a potential target for anti-cancer drugs. A better understanding of the cellular processes controlled by Aurora B thus contributes to optimize the efficiency and specificity of cytostatic treatments.

EXPERIMENTAL PROCEDURES

Cell Lines and Plasmids

HeLa, hTERT-RPE1, and NRK cells were cultured in DMEM (GIBCO) supplemented with 10% fetal calf serum (PAA Laboratories) and 1% Penicillin/Streptomycin (Invitrogen), and grown on LabTek chambered coverslips (Nunc) for live microscopy. All live imaging experiments using HeLa or hTERT-RPE1 cells were performed with monoclonal cell lines stably expressing combinations of the fluorescent markers as indicated throughout the manuscript (complete lists of plasmids and cell lines see Tables S1 and S2).

Microscopy and Image Analysis

Confocal live imaging was on a customized Zeiss LSM 510 Axiovert microscope using a 63×, 1.4 N.A. Oil Plan-Apochromat or 40×, 1.3 N.A. Oil EC Plan-Neofluar objective (Zeiss), or on a Zeiss Axiovert equipped with a VisiTech Spinning disk and Hamamatsu ORCA ER camera and a 100×, 1.4 N.A. Oil Plan-Apochromat objective (Zeiss). Both microscopes were equipped with piezo focus drives (piezosystemjena), custom-designed filters (Chroma), and EMBL incubation chambers (European Molecular Biology Laboratory), providing a humidified atmosphere at 37°C with 5% CO_2. Long-term movies for Figures 1B–1E were acquired on a Molecular Devices ImageXpressMicro microscope, equipped with incubation chamber (37°C, humidified, 5% CO_2) and a 10×, 0.5 N.A. S Fluor objective (Nikon). Sample illumination was generally kept to a minimum and had no adverse effect on cell division and proliferation. Image analysis was by Zeiss LSM510 and ImageJ software. Linear contrast adjustments were applied with constant settings for different experimental conditions. For quantification of antibody stainings, 3D image stacks were projected by mean fluorescence intensity. Background-subtracted intensity was then measured in a region of constant size centered around the peak fluorescence signal at midbodies, or chromosome bridges.

Photoactivation and Photobleaching

For experiments shown in Figures 2C and 2D, S2 and 5E, PAGFP was activated by radiating a defined region with 30 mW 405 nm diode laser at 100% transmission. Activation of PAGFP on the PALM microscope (Figures 2F–2H) was by UV epifluorescence illumination through the closed field aperture for about 1 s. FRAP experiments used 50 iterations of photobleaching at 100% transmission of 488 nm laser at regions similar to the one indicated in Figure 6E. Recovery kinetics of mean fluorescence intensity were measured in a region of constant size at the location of the Aurora B ring, and after background subtraction were normalized to pre- and first postbleach frame. Fluorescence loss in photobleaching experiments used 20 iterations of photobleaching at 100% transmission of 488 nm laser at regions similar to the one indicated in Figure 6G before acquisition of each time point. Mean fluorescence was measured in regions of constant size as indicated in Figure 6G, and after background subtraction normalized to the prebleach frame.

Laser Microsurgery

Intracellular Microsurgery was performed on a PALM MicroLaser System (Zeiss) equipped with a pulsed 355 nm UV-A laser using a 100 × 1.3NA Oil DICIII EC Plan NeoFluar objective (Zeiss). The microsurgery protocol was applied by focused laser illumination during linear stage movement as highlighted in the respective Figs. The following parameters were set: 45% laser energy, 63% laser focus, 14% cut speed. Cells exposed to laser microsurgery were viable at least 2 hr after microsurgery, tested by DIC imaging.

Inhibitor and Asbestos Treatments

For immunofluorescence inhibitors were added directly after mitotic shake-off and the cells were fixed and stained after 2–3 hr incubation. For time-lapse imaging experiments inhibitors were added during telophase. DMSO (Sigma-Aldrich), Hesperadin (kind gift of N. Kraut, Boehringer Ingelheim, final concentration: 100 nM), ZM1 (Tocris, final concentration: 2–4 μM), RO-3306 (Calbiochem, final concentration: 30 μM), and SB203580 (Calbiochem, final concentration: 10 μM) were dissolved in prewarmed culture medium to 10x solutions, and added to their final concentrations. Crocidolite (UICC Asbestos Standards) fibers of 90-260 nm diameter (spi supplies, USA; (Pelin et al., 1992)) were added to the cell at a final concentration of 5 $\mu g/cm^2$ followed by incubation for 12–24 hr.

Immunofluorescence Staining

Immunofluorescence and phalloidin stainings were by standard methods after formaldehyde or methanol fixation. Mouse anti-LAP2 (BD Transduction Laboratories), rabbit anti-Mklp1 (Santa Cruz Biotechnology), rabbit anti-phospho-S911-Mklp1 (kind gift from F. Barr), rabbit anti-Aurora B (kind gift of P. Meraldi), rabbit anti- phospho-T232-Aurora B (Rockland), and rabbit anti-INCENP (Abcam) were used as primary antibodies, and appropriate secondary antibodies conjugated with either Alexa-Fluor 405, Alexa-Fluor 488, Alexa-Fluor 546 or Alexa-Fluor 633 (Invitrogen) were used. Actin was visualized by incubation with 5 U/ml Alexa Fluor 546 or 488 Phalloidin (Invitrogen) for 1 hr.

SUPPLEMENTAL DATA

Supplemental Data include Supplemental Experimental Procedures, two tables, six figures, Supplemental References, and fifteen movies and can be found with this article online at http://www.cell.com/supplemental/S0092-8674(08)01601-2.

ACKNOWLEDGMENTS

We thank Y. Barral and M. Mendoza for communicating unpublished results and critical reading of the manuscript; and C. Rieder, M. Peter, U. Kutay, H. Meyer, P. Meraldi, S. Trautmann, P. Lenart, and M. Petronczki for helpful discussions. We thank G. Csucs and J. Kusch from the light microscopy

center (LMC) for technical support; and N. Kraut for providing Hesperadin; U. Kutay and P. Muhlhausser for mRFP-LAP2β plasmid and cells expressing H2B-mRFP and EGFP-LAP2β; R.Y. Tsien for mRFP, mCherry, and MyrPalm-EYFP; J. Lippincott-Schwartz for mEGFP and PAGFP; L. Yu for Aurora B-EGFP; J. Ellenberg for H2B-mRFP; S. Wiemann for Mklp1-YFP; M.C. Cardoso for mRFP-PCNA plasmid; P. Meraldi for Aurora B antibody; F.A. Barr for phospho-S911-Mklp1 antibody; S. Narumiya for HeLa "Kyoto" cells; and J. Pines for hTERT-RPE1 cells. This work was supported by SNF research grant 3100A0-114120, a European Young Investigator (EURYI) award of the European Science Foundation, and an MBL Summer Research Fellowship to D.G., a postdoctoral fellowship of the German Science Foundation (DFG) to P.S., a Roche Ph.D. fellowship to M.S, and a Mueller fellowship of the Molecular Life Sciences Ph.D. program Zurich to M.H.

Received: May 22, 2008
Revised: September 24, 2008
Accepted: December 5, 2008
Published: February 5, 2009

REFERENCES

Acilan, C., Potter, D.M., and Saunders, W.S. (2007). DNA repair pathways involved in anaphase bridge formation. Genes Chromosomes Cancer *46*, 522–531.

Caldwell, C.M., Green, R.A., and Kaplan, K.B. (2007). APC mutations lead to cytokinetic failures in vitro and tetraploid genotypes in Min mice. J. Cell Biol. *178*, 1109–1120.

Chan, K.L., North, P.S., and Hickson, I.D. (2007). BLM is required for faithful chromosome segregation and its localization defines a class of ultrafine anaphase bridges. EMBO J. *26*, 3397–3409.

Chestukhin, A., Pfeffer, C., Milligan, S., DeCaprio, J.A., and Pellman, D. (2003). Processing, localization, and requirement of human separase for normal anaphase progression. Proc. Natl. Acad. Sci. USA *100*, 4574–4579.

Chin, K., de Solorzano, C.O., Knowles, D., Jones, A., Chou, W., Rodriguez, E.G., Kuo, W.L., Ljung, B.M., Chew, K., Myambo, K., et al. (2004). In situ analyses of genome instability in breast cancer. Nat. Genet. *36*, 984–988.

Cimini, D., Mattiuzzo, M., Torosantucci, L., and Degrassi, F. (2003). Histone hyperacetylation in mitosis prevents sister chromatid separation and produces chromosome segregation defects. Mol. Biol. Cell *14*, 3821–3833.

Eggert, U.S., Mitchison, T.J., and Field, C.M. (2006). Animal cytokinesis: from parts list to mechanisms. Annu. Rev. Biochem. *75*, 543–566.

Fujiwara, T., Bandi, M., Nitta, M., Ivanova, E.V., Bronson, R.T., and Pellman, D. (2005). Cytokinesis failure generating tetraploids promotes tumorigenesis in p53-null cells. Nature *437*, 1043–1047.

Ganem, N.J., Storchova, Z., and Pellman, D. (2007). Tetraploidy, aneuploidy and cancer. Curr. Opin. Genet. Dev. *17*, 157–162.

Girdler, F., Gascoigne, K.E., Eyers, P.A., Hartmuth, S., Crafter, C., Foote, K.M., Keen, N.J., and Taylor, S.S. (2006). Validating Aurora B as an anti-cancer drug target. J. Cell Sci. *119*, 3664–3675.

Gisselsson, D., Pettersson, L., Hoglund, M., Heidenblad, M., Gorunova, L., Wiegant, J., Mertens, F., Dal Cin, P., Mitelman, F., and Mandahl, N. (2000). Chromosomal breakage-fusion-bridge events cause genetic intratumor heterogeneity. Proc. Natl. Acad. Sci. USA *97*, 5357–5362.

Glotzer, M. (2005). The molecular requirements for cytokinesis. Science *307*, 1735–1739.

Guse, A., Mishima, M., and Glotzer, M. (2005). Phosphorylation of ZEN-4/MKLP1 by aurora B regulates completion of cytokinesis. Curr. Biol. *15*, 778–786.

Hauf, S., Cole, R.W., LaTerra, S., Zimmer, C., Schnapp, G., Walter, R., Heckel, A., van Meel, J., Rieder, C.L., and Peters, J.M. (2003). The small molecule Hesperadin reveals a role for Aurora B in correcting kinetochore-microtubule attachment and in maintaining the spindle assembly checkpoint. J. Cell Biol. *161*, 281–294.

Jensen, C.G., Jensen, L.C., Rieder, C.L., Cole, R.W., and Ault, J.G. (1996). Long crocidolite asbestos fibers cause polyploidy by sterically blocking cytokinesis. Carcinogenesis *17*, 2013–2021.

Kelly, A.E., Sampath, S.C., Maniar, T.A., Woo, E.M., Chait, B.T., and Funabiki, H. (2007). Chromosomal enrichment and activation of the aurora B pathway are coupled to spatially regulate spindle assembly. Dev. Cell *12*, 31–43.

Keppler, A., Arrivoli, C., Sironi, L., and Ellenberg, J. (2006). Fluorophores for live cell imaging of AGT fusion proteins across the visible spectrum. Biotechniques *41*, 167–170, 172, 174–165.

Leonhardt, H., Rahn, H.P., Weinzierl, P., Sporbert, A., Cremer, T., Zink, D., and Cardoso, M.C. (2000). Dynamics of DNA replication factories in living cells. J. Cell Biol. *149*, 271–280.

Maser, R.S., and DePinho, R.A. (2002). Connecting chromosomes, crisis, and cancer. Science *297*, 565–569.

Muhlhausser, P., and Kutay, U. (2007). An in vitro nuclear disassembly system reveals a role for the RanGTPase system and microtubule-dependent steps in nuclear envelope breakdown. J. Cell Biol. *178*, 595–610.

Mullins, J.M., and Biesele, J.J. (1977). Terminal phase of cytokinesis in D-98s cells. J. Cell Biol. *73*, 672–684.

Neef, R., Klein, U.R., Kopajtich, R., and Barr, F.A. (2006). Cooperation between mitotic kinesins controls the late stages of cytokinesis. Curr. Biol. *16*, 301–307.

Norden, C., Mendoza, M., Dobbelaere, J., Kotwaliwale, C.V., Biggins, S., and Barral, Y. (2006). The NoCut pathway links completion of cytokinesis to spindle midzone function to prevent chromosome breakage. Cell *125*, 85–98.

Patterson, G.H., and Lippincott-Schwartz, J. (2002). A photoactivatable GFP for selective photolabeling of proteins and cells. Science *297*, 1873–1877.

Pelin, K., Husgafvel-Pursiainen, K., Vallas, M., Vanhala, E., and Linnainmaa, K. (1992). Cytotoxicity and Anaphase Aberrations induced by Mineral Fibres in Cultured Human Mesothelial Cells. Toxicol. In Vitro *6*, 445–450.

Rosasco-Nitcher, S.E., Lan, W., Khorasanizadeh, S., and Stukenberg, P.T. (2008). Centromeric Aurora-B activation requires TD-60, microtubules, and substrate priming phosphorylation. Science *319*, 469–472.

Ruchaud, S., Carmena, M., and Earnshaw, W.C. (2007). Chromosomal passengers: conducting cell division. Nat. Rev. Mol. Cell Biol. *8*, 798–812.

Shi, Q., and King, R.W. (2005). Chromosome nondisjunction yields tetraploid rather than aneuploid cells in human cell lines. Nature *437*, 1038–1042.

Stewenius, Y., Gorunova, L., Jonson, T., Larsson, N., Hoglund, M., Mandahl, N., Mertens, F., Mitelman, F., and Gisselsson, D. (2005). Structural and numerical chromosome changes in colon cancer develop through telomere-mediated anaphase bridges, not through mitotic multipolarity. Proc. Natl. Acad. Sci. USA *102*, 5541–5546.

Uetake, Y., and Sluder, G. (2004). Cell cycle progression after cleavage failure: mammalian somatic cells do not possess a "tetraploidy checkpoint". J. Cell Biol. *165*, 609–615.

Weaver, B.A., Silk, A.D., and Cleveland, D.W. (2006). Cell biology: nondisjunction, aneuploidy and tetraploidy. Nature *442*, E9–E10.

Yan, X., Cao, L., Li, Q., Wu, Y., Zhang, H., Saiyin, H., Liu, X., Zhang, X., Shi, Q., and Yu, L. (2005). Aurora C is directly associated with Survivin and required for cytokinesis. Genes Cells *10*, 617–626.

Yasui, Y., Urano, T., Kawajiri, A., Nagata, K., Tatsuka, M., Saya, H., Furukawa, K., Takahashi, T., Izawa, I., and Inagaki, M. (2004). Autophosphorylation of a newly identified site of Aurora-B is indispensable for cytokinesis. J. Biol. Chem. *279*, 12997–13003.

Zacharias, D.A., Violin, J.D., Newton, A.C., and Tsien, R.Y. (2002). Partitioning of lipid-modified monomeric GFPs into membrane microdomains of live cells. Science *296*, 913–916.